MODELLING THE CARBONATION REACTIONS IN SELF-HEALING CONCRETE

E. JAVIERRE[*], F.J. GASPAR[†] AND C. RODRIGO[†]

[*]Centro Universitario de la Defensa
Zaragoza, Spain
e-mail: etelvina@unizar.es

[†]Universidad de Zaragoza
Zaragoza, Spain
e-mail: [fjgaspar,carmenr]@unizar.es

Key words: Autogeneous Healing Reactions, Reactive Flow, Unsaturated Porous Media, Porosity Evolution

Abstract. This work focuses on the coupling of the self-healing chemical reactions with the reactive flow in unsaturated concrete materials, using the carbonation of $Ca(OH)_2$ as a prototype reaction model. The multi-component flow model couples the concentration of the reactant ($Ca(OH)_2$) and external triggers (moisture and CO_2) with the local remodeling of the matrix based on linear dissolution and precipitation reaction kinetics. The model reproduces the main features of the carbonation reaction and predicts the decrease in matrix porosity due to the self-healing mechanism.

1 INTRODUCTION

Self-repair of small cracks in concrete can be achieved by the precipitation of minerals at the crack surfaces. This basic process occurs during the hydration of unhydrated particles in young concrete, the carbonation reactions in late-age concrete, or the activation of latent bacteria within the concrete matrix [1]. Depending on the conditions, several of these mechanisms can combine over time. The reactants (C_2S, C_3S, CSH, $Ca(OH)_2$, bacteria ...) require the presence of a trigger to activate the precipitation reaction. Depending on the self-healing mechanism, the trigger may be acquired externally (moisture, CO_2, ...) or be internally loaded (lactate in the case of encapsulated bacteria).

The $Ca(OH)_2$ carbonation reaction is considered here as a prototype model. It is reported that the crack width that can be sealed by this mechanism is limited (up to 300 μm, [1]),

but it shares several common features with the above-described reaction mechanisms and it is well documented in the literature [2–6]. Moreover, the progress of the carbonation reactions is directly connected with the durability of reinforced concrete [7, 8].

The healing reactions dynamically change the microstructure of the material, and hence its permeability and the transport of chemicals. This crucial feature has been addressed in terms of an evolving porosity, regarding the hydration degree in young concretes [9] and the volume of the newly formed calcite precipitates [2] and/or its precipitation rate [3] in late-age concretes. The volume of the newly formed calcite precipitates has also been used recently [5], in the spirit of the continuum damage-healing models, to define a healing variable based on the physico-chemical processes at the microscopic scale.

This work focuses on the coupling of the

$Ca(OH)_2$ carbonation reaction with the flow and reactive transport through a partly saturated porous medium. In that sense, the proposed model extends the detailed physico-chemical description of the carbonation reaction [3, 8, 11] with the reactive flow model in porous media, in line with that presented in [6]. Moreover, this paper extends [6] with a more physically sound approximation to the application problem. The model predicts the evolution of moisture, carbon dioxide, portlandite, calcite and the porosity throughout the concrete sample. This information may be used to build estimates of the healing capacity of the system, as well as to obtain indicators of changes in the pH that directly couple with the corrosion risk in reinforced concrete.

The remainder of the paper is organized as follows. First a detailed description of the physico-chemical model of the $Ca(OH)_2$ carbonation reaction will be given. Subsequently the complete mathematical model, based on macroscopic conservation equations of the chosen variables, will be presented. The numerical solution method will be described next. The paper is completed with the presentation of a general test case and the conclusions.
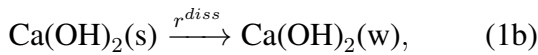
2 $Ca(OH)_2$ CARBONATION REACTION

The carbonation reaction requires the presence of moisture and carbon dioxide, and its elementary steps can be summarized as follows: (1) the phase change of absorbed CO_2:
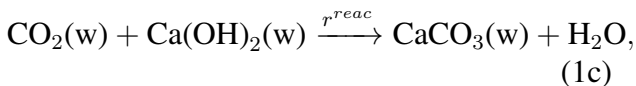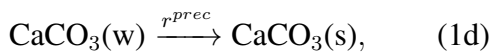
$$CO_2(g) \xrightarrow{r^{ch}} CO_2(w), \qquad (1a)$$
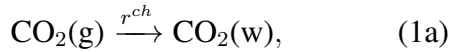
(2) the dissolution of $Ca(OH)_2$:

$$Ca(OH)_2(s) \xrightarrow{r^{diss}} Ca(OH)_2(w), \qquad (1b)$$

(3) the carbonation of the dissolved $Ca(OH)_2$:

$$CO_2(w) + Ca(OH)_2(w) \xrightarrow{r^{reac}} CaCO_3(w) + H_2O, \qquad (1c)$$

(4) the precipitation of the dissolved $CaCO_3$:

$$CaCO_3(w) \xrightarrow{r^{prec}} CaCO_3(s), \qquad (1d)$$

where r^a denotes the rate of reaction a.

For the sake of the presentation, we will denote by c_i the mass concentration ($\mathrm{kg/m^3}$) of the ith species in the reactions (1), as summarized in Table 1.

Table 1: Chemical compounds in the reactive flow model.

Index i	Compound i	Index i	Compound i
1	$CO_2(g)$	2	$CO_2(w)$
3	$Ca(OH)_2(s)$	4	$Ca(OH)_2(w)$
5	$CaCO_3(w)$	6	$CaCO_3(s)$

The mass transfer during CO_2 dissolution, reaction (1a), is governed by Henry's law

$$r^{ch} = k^{ex} \left(K^{Hen} c_1 - c_2 \right), \qquad (2)$$

where k^{ex} denotes the rate constant and K^{Hen} the Henry constant. Reported numerical results [3] show a fast CO_2 mass transfer between the gas and liquid phases. Under the hypothesis of *instantaneous* mass transfer [6], as shall be assumed hereafter, the concentrations c_1 and c_2 fulfill $K^{Hen} c_1 - c_2 = 0$.

The carbonation reaction (1c) requires the presence of moisture and carbon dioxide. Following [4] we take the kinetics of reaction (1c) to be given by:

$$r^{reac} = k^{reac} g^{hum}(RH) c_2 c_4, \qquad (3)$$

where k^{reac} denotes the reaction constant and g^{hum} denotes a moisture-dependent multiplicative factor [11] given by

$$g^{hum}(RH) = \begin{cases} 0, & \text{if } RH < 0.5, \\ \frac{RH - 0.5}{0.4}, & \text{if } 0.5 \leq RH < 0.9, \\ 1, & \text{if } 0.9 \leq RH. \end{cases}$$

The relative humidity RH can be computed using the Kelvin-Laplace law

$$RH = \exp \left(-\frac{p_c M_w}{\rho_w RT} \right),$$

where p_c denotes the capillary pressure, M_w the molar mass of water, ρ_w the density of water, R the universal gas constant and T the temperature.

Following [6], we consider linear dissolution and precipitation kinetics. The rates of reactions (1b) and (1d) are given, respectively, by

$$r^{diss} = k^{diss}\left(c^{eq}_{Ca(OH)_2} - c_4\right), \qquad (4)$$

$$r^{prec} = k^{prec}\left(c_5 - c^{eq}_{CaCO_3}\right), \qquad (5)$$

where k^{diss} and k^{prec} denote the rate constant of the dissolution and precipitation reactions and $c^{eq}_{Ca(OH)_2}$ and $c^{eq}_{CaCO_3}$ denote the equilibrium (saturation) concentration of $Ca(OH)_2$ and $CaCO_3$ respectively.
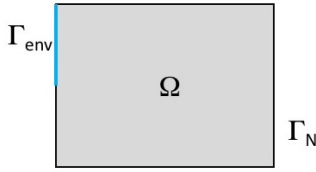

Figure 1: Sketch of the computational domain.

3 GOVERNING EQUATIONS

Let us consider a domain of computation Ω with boundary $\Gamma = \partial\Omega$, which we can write as $\Gamma = \Gamma_{env} \cup \Gamma_N$ with $\Gamma_{env} \cap \Gamma_N = \emptyset$. The concrete sample Ω is exposed to the environment through Γ_{env}, whereas it remains sealed on Γ_N (see Fig. 1). Hence, Γ_{env} may represent the surface of an open crack through which the required CO_2 and moisture can access the domain.

In the remaining of the model, ϕ will denote the porosity of the material, S_w the degree of saturation of the water phase and p the fluid pressure. Furthermore we will assume that the CO_2 mass transfer between the gaseous and fluid phases is sufficiently fast, which allows to uncouple the evolution of $CO_2(g)$ of the rest of chemical species [6]. Hence, the concentration c_1 will not be consider in the solution procedure and the boundary conditions for c_2 will take into account both the environmental conditions and Henry's law.

3.1 Conservation of the fluid phase

The flow of the fluid phase is governed by the Richards' equation. At this point we do

not take into consideration the exothermic nature of the carbonation reaction [7], and assume that the air phase remains at constant pressure (i.e. $p_c = -p$). Recalling that reaction (1c) produces water, the macroscopic conservation equation for the fluid phase can be written as:

$$\frac{\partial}{\partial t}(\phi S_w) - \nabla \cdot (K_w \nabla p) = \frac{M_w \phi S_w r^{reac}}{\rho_w}, \quad (6)$$

where K_w denotes the hydraulic permeability of the material. Notice that the gravity effects on the fluid flow have been disregarded in (6). The hydraulic permeability of the material is given by $K_w = k_{ws}k_{rw}/\mu_w$ where k_{ws} denotes the permeability of the saturated porous material, μ_w the viscosity of water, and k_{rw} denotes the relative permeability of the material. The following van Genuchten constitutive relations are used:

$$S_w(p) = \frac{1}{(1 + (-\alpha p)^n)^m}, \qquad (7a)$$

$$k_{rw}(S_w) = \sqrt{S_w}\left[1 - \left(1 - S_w^{1/m}\right)^m\right]^2, \quad (7b)$$

where $m = 1 - \frac{1}{n}$.

In the remaining of the paper we will denote by $\mathbf{q} = -K_w \nabla p$ the flux of the fluid phase.

3.2 Conservation of dissolved compounds

The dissolved compounds are subjected to both random diffusion within the fluid and passive drag due to the fluid flow. The net production of the compounds takes into account the stoichiometry of the carbonation reaction (1c) and the molar mass M_{ch} of the involved chemical compounds. Thus, we have the following macroscopic conservation equations.
Conservation of $CO_2(w)$:

$$\frac{\partial}{\partial t}(\phi S_w c_2) - \nabla \cdot (D_2 \phi S_w \nabla c_2 - \mathbf{q}c_2) =$$
$$= -M_{CO_2}\phi S_w r^{reac}. \qquad (8a)$$

Conservation of $Ca(OH)_2(w)$:

$$\frac{\partial}{\partial t}(\phi S_w c_4) - \nabla \cdot (D_4 \phi S_w \nabla c_4 - \mathbf{q}c_4) =$$
$$= \phi S_w\left(r^{diss} - M_{Ca(OH)_2}r^{reac}\right). \quad (8b)$$

Conservation of CaCO$_3$(w):

$$\frac{\partial}{\partial t}\left(\phi S_w c_5\right) - \nabla \cdot \left(D_5 \phi S_w \nabla c_5 - \mathbf{q} c_5\right) =$$
$$= \phi S_w \left(M_{CaCO_2} r^{reac} - r^{prec}\right). \quad (8c)$$

3.3 Conservation of solid compounds

The macroscopic conservation equations for the solid compounds of the model account for the dissolution and precipitation kinetics.
Conservation of Ca(OH)$_2$(s):

$$\frac{\partial}{\partial t}\left((1-\phi)c_3\right) = -(1-\phi)r^{diss}. \quad (9a)$$

Conservation of CaCO$_3$(s):

$$\frac{\partial}{\partial t}\left((1-\phi)c_6\right) = (1-\phi)r^{prec}. \quad (9b)$$

3.4 Porosity evolution

The porosity of the solid matrix is dynamically changed by the dissolution and precipitation steps. Here we assume a linear remodeling of the matrix in line with [2], taking into account the variations with respect to the initial concentrations of the solid compounds. Thus, we consider:

$$\phi = \phi_0 + \Delta_{diss}\phi - \Delta_{prec}\phi, \quad (10)$$
$$\Delta_{diss}\phi = \frac{c_3^0 - c_3}{\rho_{Ca(OH)_2}}, \quad \Delta_{prec}\phi = \frac{c_6 - c_6^0}{\rho_{CaCO_3}},$$

where ρ_{ch} denotes the density of the solid compound ch.

4 NUMERICAL SOLUTION

The model equations (6), (8), (9) and (10), supplemented with the corresponding initial and boundary conditions, are discretized in time with a one step time marching method and in space with standard Q1 finite elements. Given the nonlinear nature of the equations, an uncoupled approximation is used. For the sake of the presentation let us consider t^n and t^{n+1} two consecutive time steps, $\Delta t = t^{n+1} - t^n$, and the porosity ϕ, the fluid pressure p and the concentrations c_2 to c_6 to be known at time t^n. The following steps are carried out sequentially to obtain the solution at time t^{n+1}.

First, the porosity is updated evaluating the right hand side of Eq. (10) at the previous time step.

Next, the fluid pressure p is updated. The production term (right hand side of Eq. (6)) is treated explicitly whereas the flow term is treated implicitly. The resulting nonlinear system of equations is solved applying the modified Picard method [10], which is globally mass conservative.

Subsequently, the concentrations c_2, c_4 and c_5 of the dissolved compounds are updated. In this case, a fully implicit time discretization scheme is used. The resulting nonlinear system of equations (due to the implicit treatment of the right hand side terms in Eqs. (8)) is solved applying a standard Picard iteration, that uncouples the variables.

Finally, the concentrations c_3 and c_6 of the solid compounds are updated using the backward Euler scheme.

5 TEST CASE

We consider a rectangular concrete sample as sketched in Fig. 1. The sample is open to the environment through the boundary Γ_{env}, where Dirichlet boundary conditions are imposed on the pressure p and the dissolved CO$_2$ concentration: $p = p^{env}$ and $c_2 = c_2^{env}$. The value p^{env} is deduced from the Kelvin-Laplace law, whereas the value $c_2^{env} = K^{Henry} c_{CO_2(g)}^{env}$ is obtained from the environmental CO$_2$ gas concentration $c_{CO_2(g)}^{env}$ under the hypothesis of instantaneous phase change. In Γ_N, no flux boundary conditions are prescribed for the pressure p and the concentration c_2. In addition, no flux boundary conditions are imposed for the species c_4 and c_5 through Γ.

The concrete sample is assumed to contain a certain amount of moisture at the initial time, S_w^0, and this value is used to define the initial pressure p^0. The initial porosity ϕ^0 and solid Ca(OH)$_2$ concentration c_3^0 can be deduced from the particular mixture under consideration. Since we are interested in the changes that the carbonation reaction produces in the matrix, the initial concentrations of the remainder

chemical species is set to zero ($c_i^0 = 0$ $^{\text{kg}}/_{\text{m}^3}$ for $i = 2, 4, 5, 6$).

The following rationale has been used to define the nonzero initial and boundary conditions. We consider the conditions described in [3] for an accelerated carbonation test. The temperature, relative humidity and CO_2 concentration ($c_{CO_2(g)}^{env}$) at the environment are set to $30°$C, 65% and 0.87 $^{\text{kg}}/_{\text{m}^3}$ respectively, which imply that $p^{env} = -63.02 \times 10^6$ Pa and $c_2^{env} = 0.71$ $^{\text{kg}}/_{\text{m}^3}$. The fluid pressure within the concrete sample is assumed to be in equilibrium with the surrounding environment, $p^0 = p^{end}$. Finally, the initial porosity and solid calcium hydroxide are set to $\phi^0 = 0.3$ and $c_3^0 = 20$ $^{\text{kg}}/_{\text{m}^3}$.

The parameters defining the van Genuchten relations (7) are taken from [12] (Portland cement mixture): $k_{ws} = 5 \times 10^{-21}$ m^2, $\alpha = 5.37 \times 10^{-8}$ Pa^{-1} and $m = 0.44$. The rate constant of the carbonation reaction $k^{reac} = 0.461$ $\frac{\text{kmol m}^3}{\text{kg}^2 \text{ day}}$ is taken from [3]. The solubilities of calcium hydroxide and calcium carbonate are $c_{Ca(OH)_2}^{eq} = 1.6$ and $c_{CaCO_3}^{eq} = 0.013$ $^{\text{kg}}/_{\text{m}^3}$ respectively. Finally, the following values are considered for the diffusion coefficients $D_2 = 10^{-9}$, $D_3 = 10^{-11}$ and $D_4 = 10^{-12}$ $^{\text{m}^2}/_{\text{s}}$ and reaction rates $k^{diss} = 0.1$ and $k^{prec} = 0.2$ $\frac{\text{kg}}{\text{m}^3 \text{day}}$.

We consider a 20×10 cm^2 concrete sample with an exposed surface Γ_{env} of 5 cm of length. Results after 2 weeks of exposure to the prescribed environmental conditions are given in Figures 2-5. A time step of $\Delta t = 12$ hours has been used. The ingress of dissolved carbon dioxide through the scratch is well visible in Figure 2. The dissolution of solid $Ca(OH)_2$ and the uptake of dissolved $Ca(OH)_2$ can be appreciated in Figure 3. The initial moisture content (recall that $p^0 < 0$) promotes the dissolution of calcium hydroxide throughout the whole matrix, while the fast carbonation reaction accounts for the rapid uptake of the dissolved calcium hydroxide in the proximity of the crack.
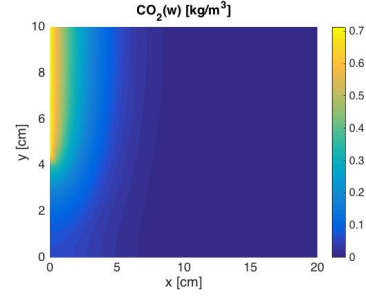

Figure 2: Concentration profile of dissolved CO_2 after 2 weeks.
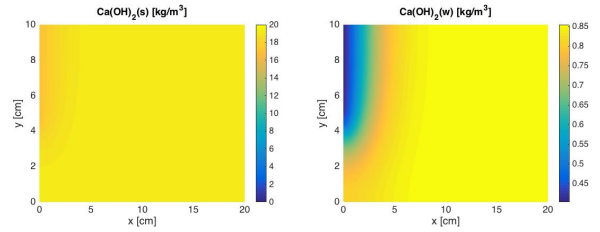

Figure 3: Concentration profiles of solid and dissolved $Ca(OH)_2$ after 2 weeks.

It should be noticed that the initial concentration of solid calcium hydroxide is far from being depleted within the considered time. Hence, the sustained supply of dissolved CO_2 and $Ca(OH)_2$ promotes the continuation of the carbonation reaction. The concentrations of the dissolved and precipitated $CaCO_3$ are presented in Figure 4. Results show the continued carbonation in vicinity of the scratch while the precipitation reaction advances through the matrix.
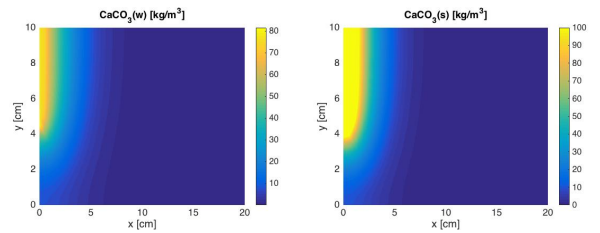

Figure 4: Concentration profiles of dissolved and solid $CaCO_3$ after 2 weeks.

Finally, the changes in the microstructure are given in Figure 5. Results clearly correlate the decrease in porosity with the newly formed precipitates of $CaCO_3$.
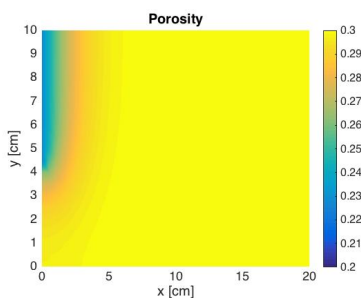
5

Figure 5: Porosity after 2 weeks.

6 CONCLUSIONS

The coupling of the physico-chemical $Ca(OH)_2$ carbonation reaction and reactive flow through an unsaturated porous material has been presented in the context of autogenous self-healing mechanisms in concrete. The model allows to estimate the course of the involved chemical compounds as well as the matrix microstructure. Thus, given the nature of the carbonation reaction, the model can be used to estimate both the localized risk of corrosion ($Ca(OH)_2$ depleted zones) and the healing capacity of the material (reductions in the porosity). The model offers a great potential to gain fine knowledge on the interplay of self-healing chemical reactions and material remodeling at the microscopic scale. The incorporation of additional chemical reactions (such as the hydration of unhydrated compounds or the production of minerals by activated bacteria) is straightforward. However, the model also presents a number of limitations. It should be remarked that an accurate estimation of certain parameters needs to be undertaken. Although the qualitative behavior of the solution reproduces the main aspects of the carbonation reaction, a detailed comparison with experimental results is necessary to supply the model with a quantitative predictive power. These are the lines of future research.

REFERENCES

[1] Van Tittelboom, K. and De Belie, N. 2013. Self-Healing in Cementitious Materials-A Review. *Materials* **6**:2182-2217.

[2] Papadakis, V.G. and Vayenas, C.G. and Fardis, M.N. 1989. A reaction engineering approach to the problem of concrete carbonation. *AIChE Journal* **35**:1639-1650.

[3] Meier, S.A. and Peter, M.A. and Muntean, A. and Böhm, M. 2007. Dynamics of the internal reaction layer arising during carbonation of concrete. *Chemical Engineering Science* **62**:1125-1137.

[4] Peter, M.A. and Muntean, A. and Meier, S.A. and Böhm, M. 2008. Competition of several carbonation reactions in concrete: A parametric study. *Cement and Concrete Research* **38**:1385-1393.

[5] Aliko-Benítez, A. and Doblare, M. and Sanz-Herrera, J.A. 2015. Chemical-diffusive modeling of the self-healing behavior in concrete. *International Journal of Solids and Structures* **69-70**:392-402.

[6] Radu, F.A. and Muntean, A. and Pop, I.S. and Suciu, N. and Kolditz, O. 2013. A mixed finite element discretization scheme for a concrete carbonation model with concentration-dependent porosity. *Journal of Computational and Applied Mathematics* **246**:74-85.

[7] Saetta, A.V., 2005. Deterioration of reinforced concrete structures due to chemical-physical phenomena: Model-based simulation. *Journal of Materials in Civil Engineering* **17**:313-319.

[8] Steffens, A. and Dinkler, D. and Ahrens, H. 2002. Modeling carbonation for corrosion risk prediction of concrete structures. *Cement and Concrete Research* **32**:93-941.

[9] Chitez, A.S. and Jefferson, A.D. 2016.A coupled thermo-hygro-chemical model for characterising autogenous healing in ordinary cementitious materials. *Cement and Concrete Research* **88**:184-197.

[10] Celia, M.A. and Bouloutas, E.T. and Zarba, R.L. 1990. A General Mass-Conservative Numerical-Solution for the Unsaturated Flow Equation. *Water Resources Research* **26**:1483-1496.

[11] Saetta, A.V. and Schrefler, B.A. and Vitaliani, R.V. 1993. The Carbonation of Concrete and the Mechanism of Moisture, Heat and Carbon-Dioxide Flow-Through Porous Materials. *Cement and Concrete Research* **23**:761-772.

[12] Chitez, A.V. 2014. Coupled Thermo-Hygro-Chemical Modelling of Self-healing Processes in Cementitious Materials. PhD Thesis, Cardiff University.